Front. Earth Sci. 2024, 18(1): 204–218
https://doi.org/10.1007/s11707-022-1053-7

RESEARCH ARTICLE

The determination of sedimentary environment and associated energy in deep-buried marine carbonates: insights from natural gamma ray spectrometry log

Jingyan LIU (✉)[1], Qian CHANG[1], Junlong ZHANG[2], Hui CHAI[3], Feng HE[4], Yizan YANG[1], Shiqiang XIA (✉)[5]

1 School of Energy Resources, China University of Geosciences (Beijing), Beijing 100083, China
2 Exploration and Development Research Institute, Daqing Oilfield Company, PetroChina, Daqing 163712, China
3 China National Oil and Gas Exploration and Development Co., Ltd (CNODC), Beijing 100032, China
4 Beijing Research Institute of Uranium Geology, Beijing 100029, China
5 College of Mining Engineering, North China University of Science and Technology, Tangshan 063210, China

Abstract It has always been challenging to determine the ancient sedimentary environment and associated energy in deep-buried marine carbonates. The energy represents the hydrodynamic conditions that existed when the carbonates were deposited. The energy includes light and chemical energies in compounds and kinetic energy in currents and mass flow. Deep-buried marine carbonates deposited during the Ordovician depositional period in the eastern Tarim Basin result from a complex interplay of tectonics, sedimentation, and diagenesis. As a result, determining the ancient sedimentary environment and associated energy is complex. The natural gamma-ray spectrometry (GRS) log (from 12 wells) is used in this paper to conduct studies on the sedimentary environment and associated energy in deep-buried marine carbonates. The findings show that the values of thorium (Th), uranium (U), potassium (K), and gamma-ray without uranium (KTh) in a natural GRS log can reveal lithological associations, mineral composition, diagenetic environment, stratigraphic water activity, and ancient climatic change. During the Ordovician, quantitative analysis and determination of sedimentary environment energy are carried out using a comprehensive calculation of natural GRS log parameters in typical wells (penetrating through the Ordovician with cores and thin sections) of well GC4, well GC6, well GC7, and well GC8. The results show that GRS log can determine different lithology associations in typical wells than a sieve residue log. Furthermore, cores and thin sections can be used to validate the determination of lithology associations. Based on the determination of lithology associations, the lithology associations that reflect the sedimentary environment and associated energy can be analyzed in a new approach. Furthermore, the sedimentary environment energy curve derived from a natural GRS log can reveal hydrodynamic fluctuations during depositional periods, which will aid in the discovery of carbonate reservoirs, establishing sequence stratigraphic frameworks, and the reconstruction of sea-level changes in the future.

Keywords ancient sedimentary environment, energy of sedimentary environment, marine deep-buried carbonates, natural GRS, the Ordovician, eastern Tarim Basin

1 Introduction

The distribution of radioactive nuclear elements in rock records, such as thorium (Th), uranium (U), and potassium (K), is linked to lithology, mineral composition, diagenesis, and groundwater activity (Guo et al., 1996; Chi, 2003; Adamu et al., 2020; Ghosal et al., 2020). Generally, sedimentary rock's Th content decreases with grain size (Zhang et al., 2006; Ghosal et al., 2020). The main factors controlling Th distribution in sedimentary rocks are clay mineral adsorption on Th and the presence of Th in stable minerals. Furthermore, Th has good chemical stability and a low migration capacity. As a result, there is a linear relationship between Th content and argillaceous deposit content in sedimentary rocks (Lima et al., 2005; Ghosal et al., 2020). Groundwater activity is closely related to increased U content in the

Received October 5, 2022; accepted January 11, 2023

E-mails: ljingyan@cugb.edu.cn (Jingyan LIU)
xiasq007@126.com (Shiqiang XIA)

permeable stratum. Because of its active chemical properties and solubility in water, U is easily migrated to the deep by groundwater along main faults or fracture zones formed in the karst or tectonically active zone. Then, it is reduced to tetravalent U and precipitated under reducing conditions. As a result, the U content has a strong relationship with hydrodynamics. Furthermore, there is a linear relationship between K concentration and argillaceous deposit concentration in sedimentary rocks. In fluvial deposits, K has a higher value than Th and U. The natural gamma-ray spectrum content of fluvial deposits is generally higher than that of carbonate deposits (Davies and Elliott, 1996; Lima et al., 2005). Furthermore, the high Th and K contents indicate a stable and low-energy humid sedimentary environment. In contrast, a high U and K contents indicate a turbulent and high-energy sedimentary environment with a dry climate (Ruffell and Worden, 2000; Wang and Zhu, 2002; Chen and Zha, 2004). According to empirical statistics, Th/U > 7 characterizes continental mudstone and bauxite, which primarily reflect continental sedimentation with complete weathering, oxidation, and leaching. When the Th/U value is between 2 and 7, it generally represents a marine sedimentary environment with a small amount of terrigenous supply. When Th/U < 2, the environment is generally marine sedimentary, with relatively deep-water and little terrigenous supply (Liu et al., 2000; Yang et al., 2003; Wang, 2004). It can be concluded that the natural gamma spectrum has beneficial effects on determining the ancient sedimentary environment.

Natural gamma-ray content, sporopollenin content, and clay mineral content are all consistent (Ehrenberg and Svana, 2001; Koptíková et al., 2010; Feng et al., 2016). Sporopollen content and clay mineral content, for example, can reveal climate and sea-level changes (Chen et al., 2001; Liu et al., 2009; Zhang, 2017). As a result, the natural gamma-ray spectrum can serve as an indicator of paleoclimate (Yang et al., 2003; Ghasemi-Nejad et al., 2010). The U, Th, K, and KTH in the natural gamma-ray spectrum can reflect energy changes in the sedimentary environment and can be used to determine the ancient sedimentary environment by combining lithology associations, conventional logs, and seismic reflections (Liu and Zhou, 2007; Yang et al., 2010; Wu et al., 2011).

Over the last few decades, research on the Ordovician sedimentary environment in the eastern Tarim Basin is still in its early stages (Lin et al., 2012, 2013; He et al., 2017). Furthermore, determining the sedimentary environment is difficult due to limitations in industry data sets and the influence of special and complicated settings in the eastern Tarim Basin. As a result, only a few investigations of the sedimentary environment were conducted. At the time, the energy of the sedimentary environment was unofficially proposed. According to previous research, there is a misunderstanding between energy and the sedimentary environment (Lin et al., 2012, 2013; Gao et al., 2016; He et al., 2017). The determination of energy has always been based on grain size analysis (Wang and Zhu, 2002; Zhao et al., 2010; Zhang et al., 2020). Owing to data limitations, conducting grain size analysis in the eastern Tarim Basin is challenging. However, previous studies using natural GRS logs to reveal changes in paleoclimate and sedimentary environment yielded fruitful results (Ruffell and Worden, 2000; Chen and Zha, 2004; Ghasemi-Nejad et al., 2010). A corresponding investigation is conducted based on the natural GRS log to better address these issues. The goal is to systematically determine the ancient sedimentary environment and associated energy in deep-buried marine carbonates. The findings of this study will guide future hydrocarbon exploration in similar sedimentary environments. Most importantly, this research aims to investigate the ratio of Th, U, and K can be used as a proxy for the ancient sedimentary environment and associated energy in deep-buried carbonate reservoirs for the first time in borehole wireline logs.

2 Geological settings

The Tarim Basin, a superimposed or multicycle basin located in north-west China, has undergone long-term tectonic evolution and has hosted numerous petroleum reserves (Fig. 1(a)) (He et al., 2005; Lin et al., 2012, 2013; Laborde et al., 2019). The Tarim Basin is 56 × 10^4 km^2 in size (Wu et al., 2002; He et al., 2005; Lin et al., 2013). The eastern Tarim Basin is bounded to the east by the Luobopo Low Rise, to the west by the Awati-Manjiaer Transition Zone and the Gucheng Low Rise, to the south by the South-eastern Depression, and to the north by the Tabei Uplift (Figs. 1(b) and 1(c)) (Han et al., 2009; Dong et al., 2014; Wu et al., 2018).The eastern Tarim Basin formed due to the interaction of subduction and collision between the Northern Tianshan Mountain, the Yining-Junggar Plate, the Eurasian Plate, the Southern Arkin, the Lhasa Block, the Qiangtang Block, and the India Plate. Therefore, the tectonic framework of the eastern Tarim Basin is complicated (Tang, et al., 2003; Han, et al., 2009). The research area, Gucheng Area, is in the south-west of the eastern Tarim Basin (Figs. 1(c) and 1(d)). It is bounded to the south by the Cheerchen Fault, to the north-east by the Manjiaer Depression, and to the north-west by the Awati-Manjiaer Transition Zone (Fig. 1(d)) (Wu et al., 2015, 2018). The coverage area is roughly 6100 km^2 (Wang et al., 2011; Wu et al., 2015). It has a broad and gentle nose-like structure with an NW strike. The southern part is heavily influenced by the Cheerchen Fault, which has resulted in a series of complex thrusting structures. In contrast, the northern part is affected only marginally by the Cheerchen Fault, with gentle structures and locally faulted anticlines (Wu et al., 2015; He et al., 2017).

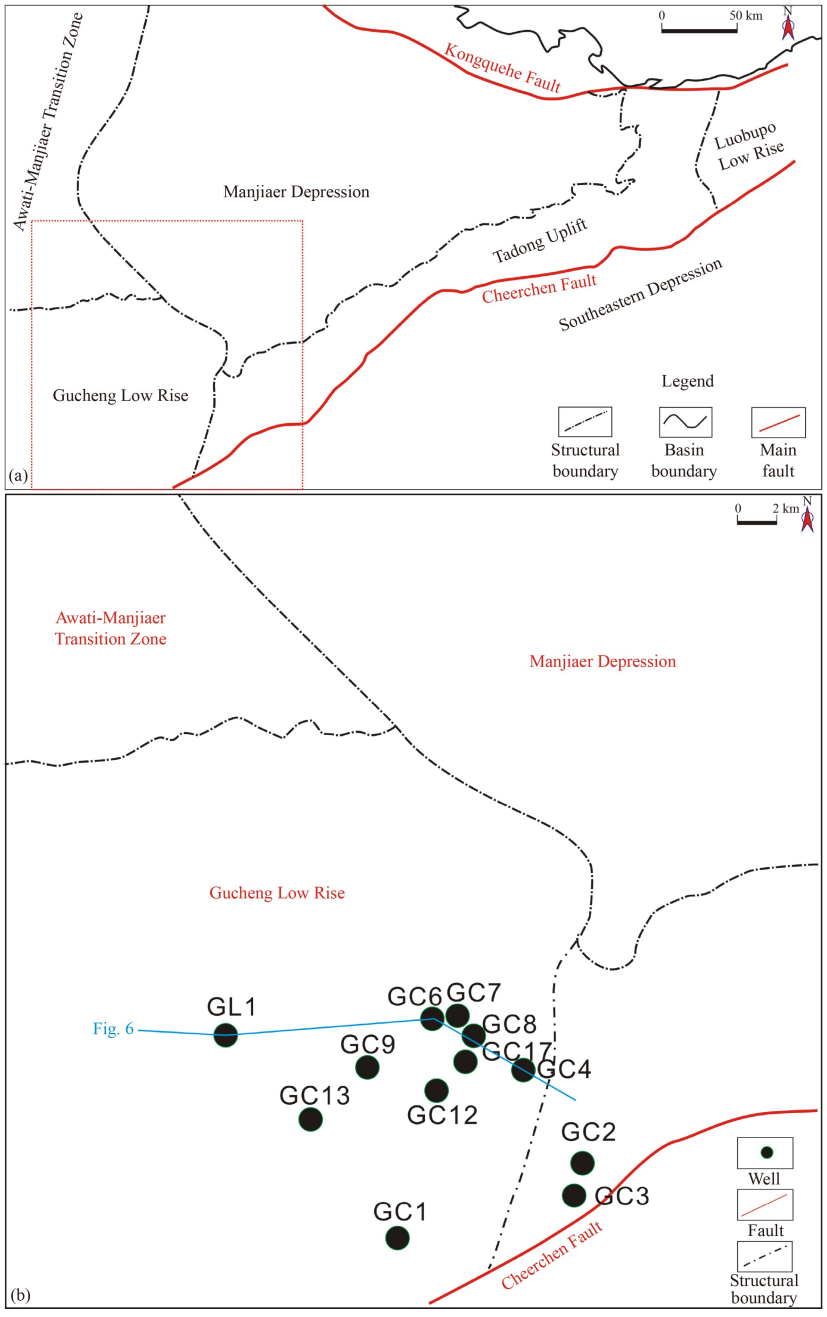

Fig. 1 (a) Showing the distribution of structural units and faults in Eastern Tarim Basin; (b) showing the wells and database used in the study area.

During the Cambrian-Middle Ordovician period, the Gucheng Area was in an extensional setting (He et al., 2017). Platform facies (mostly restricted platform, semi-restricted platform, and open platform) and platform marginal facies (mostly foreslope) predominated (Wang et al., 2014a; He et al., 2016). The lithology included dolomite, limy dolomite, and limestone. The influence of the first episode of tectonic movement in the middle Caledonian eroded the top of the Middle Ordovician. Sea level rose rapidly in the Early Ordovician, resulting in deep-water basin facies (primarily neritic shelf and shelf slope) (Wang et al., 2011; Wang et al., 2014b). The Gucheng Area was influenced by the third episode of tectonic movement in the middle Caledonian, which resulted in a high in the south and a low in the north. Lower Ordovician Penglaiba Formation, Lower-Middle Ordovician Yingshan Formation, Middle Ordovician Yijianfang Formation, Upper Ordovician Tumuxiuke Formation, and Upper Ordovician Queerqueke Formation are the main Ordovician strata preserved in the Gucheng Area, eastern Tarim Basin (Fig. 2) (Feng et al., 2007; Lin et al., 2012, 2013; Wu et al., 2015). Dolomitic limestone,

granular dolomite, and limy dolomite dominate the Penglaiba Formation, with thicknesses ranging from 120 m to 300 m (Wu et al., 2015). The Yingshan Formation is divided into two sections with thicknesses ranging from 370 to 990 m (Fig. 2) (Lin et al., 2012; Zhang et al., 2021). The lower section comprises granular dolomite, limy dolomite, and dolomitic limestone, while the upper section comprises calcarenite, micrite, and dolomitic limestone (Fig. 2) (Zhang et al., 2021). The Yijianfang Formation is composed primarily of calcarenite and granular limestone with thicknesses ranging from 70 to 190 (Fig. 2) (Wu et al., 2015; Zhang et al., 2021). The Tumuxiuke Formation is primarily composed of argillaceous limestone with a maximum thickness of 50 m (Fig. 2). The Queerqueke Formation contains the thickest sandstone and mudstone, ranging in thickness from 1200 to 2400 m (Fig. 2) (Wu et al., 2015; Zhang et al., 2021).

3 Database and methodology

3.1 Database

The data sets are obtained from the Exploration and Development Research Institute, Daqing Oilfield Company, PetroChina. The data sets predominantly include wireline logs, 2D seismic lines, sieve residue logs, core photos and thin sections. The wireline logs (from 12 wells) primarily consist of DT, GR, and PE logs with a sampling rate of 0.125 m. The DT log is used to determine the lithology and porosity. The GR log is used to detect radioactivity in lithology associations. The purity of lithology and its associations are determined using the PE log. Furthermore, natural GRS logs are collected from boreholes using a portable device. A single pristine NaI crystal is commonly used in the device, surrounded by oscillation detectors. The crystal's design allows for continuous documentation of the gamma-ray hit number on the crystal. Furthermore, the device enables analysts to differentiate the intensity of radioactive element sources that emit light pulses. The hitting energy is then converted in a photomultiplier tube by splitting the intensity of the light pulse into the corresponding voltage pulse of the original gamma-ray energy. Borehole gamma-ray spectrometers are intended for use in natural sedimentary environments to analyze the most common radioactive elements (Th, U, and K). As a result, the spectroscope's numerical value is equivalent, but not identical, to other common methods of gamma-ray radiation or elemental abundance. Alternatively, the devices for measuring radioactive intensity have been in use for a long time. The numerical value has been calibrated in terms of errors and deviations from the API standard. The study area is traversed by 553 km of 2D seismic lines with a dominant frequency of 30 Hz. The sieve residue logs (from 12 wells) were sampled every 5 m. Every 100 m, the lag time is measured. The core images are from wells scattered throughout the Gucheng Low Rise, primarily wells GC 4, 6, 7, and 8. The total length of these well cores are approximately 35.1 m. The thin sections are performed at the Tarim Oilfield Company's test center using a Germany Zeiss microscope with different digital zoom scales.

3.2 Methodology

3.2.1 The theory for determining ancient sedimentary environment and associated energy

The integrated superposition method seeks to conduct integrated and quantitative analysis by using multiple typical parameters derived from natural GRS logs. The superimposition process begins with the analysis of typical individual parameters, followed by the superimposition and combination of the results of each parameter into the final results. Unlike the previous method, in which each typical parameter is first superimposed and then analyzed, the integrated superimposition method can fully exploit the role of each parameter during the analysis process, while the final parameters are well integrated, making the determination results more objective and accurate. With the help of cores and thin sections, the integrated superimposition method can best use every typical parameter to determine and finally quantify the energy of the sedimentary environment in ancient deep-buried carbonate reservoirs.

3.2.2 The optimization for parameters in determining the ancient sedimentary environment and associated energy

In natural GRS, the ratio of numerical values (Th, U, and K) is calculated as Th/U, U/(U + K + Th), Th/(U + K + Th), Th/KTh, U/(Th + K), Th/K, K/(U + Th), U-K, U/(Th + K)-Th/KTh, U/(Th + K)-Th/KTh + U-K. The calculated ratios and the original data are then optimized to calibrate the energy based on the integrated analysis of cores and thin sections. Finally, the parameters that correspond well with changes in the sedimentary environment and associated energy are chosen for characterization. The final optimized parameters primarily include U-K, U/(Th + K)-Th/KTh (referred to as Parameter 1/P1), U/(Th + K)-Th/KTh + U-K (referred to as Parameter 2/P2), Th/U, PE.

4 Results and interpretations

4.1 Determination of energy

The cores and thin sections aid in determining multiple energies in the sedimentary environment, as well as the

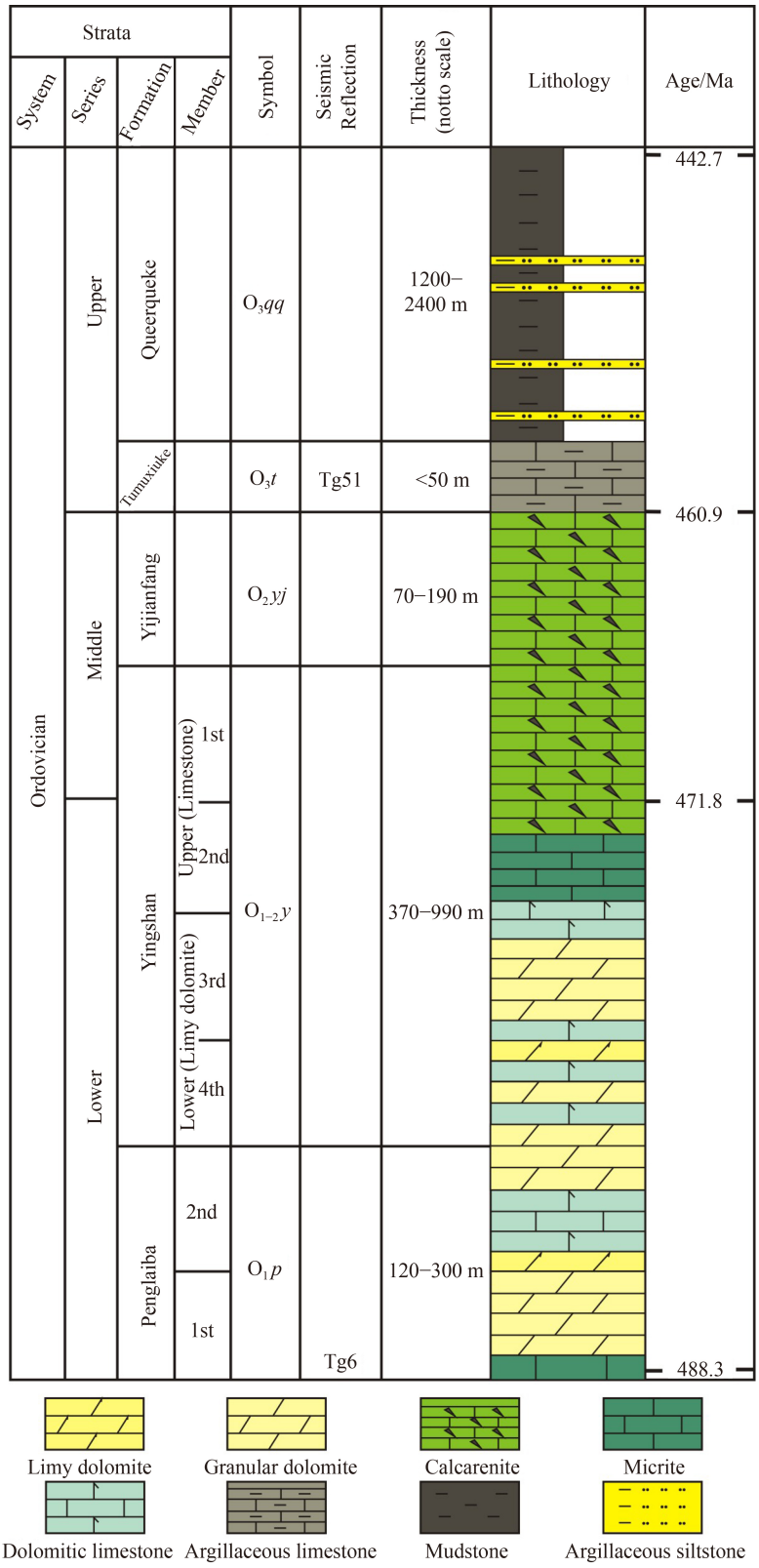

Fig. 2 The stratigraphic column of the Ordovician in eastern Tarim Basin (cited and integrated from Research Institute of Petroleum Exploration and Development, PetroChina, Wu et al. (2015), Zhang et al. (2021); the thickness is designed not to scale).

calibration of typical wireline parameters in various energy sections. Then, in conjunction with changes in parameters and borehole conditions, a standard for determining energy resulting from wireline parameters can be established (Table 1).

Different boreholes may have slightly different

determination standards. However, the values in the determination standard can be slightly adjusted to changes in parameters and borehole conditions. This method is found to be ineffective in determining the energy of dolomite. Therefore, the dolomite is identified before the limestone energy determination. The specifics are as follows. To begin, the PE values are used to differentiate between dolomite and limestone. The energy of the limestone is then calculated. The GRS parameters (including U-K, parameter 1/P1, parameter 2/P2, and Th/U) are used to determine low, medium, and high energy. Finally, all parameters are determined, and the results are displayed (Table 2). The table shows the determination results in some depth sections of well GC7. It is concluded that the results are highly comprehensive, avoiding discrimination of individual parameters and quantitatively determining energy changes.

Table 1 The standard for determination of energy resulted from parameters

Energy	Th/U(FRAC)	U-K/ppm	P1/ppm	P2/ppm
Low energy	>0.8	<0.4	<1	<1.1
Medium energy	0.3–0.8	0.4–1.1	1–2.1	1.1–2.7
High energy	<0.3	>1.1	>2.1	>2.7

Notes: U/(Th+K)-Th/KTh (referred to as Parameter 1/P1); U/(Th+K)-Th/KTh+ U-K (referred to as Parameter 2/P2); PE indicates electron density index. U, Th, K indicates corresponding content of radioactive elements.

The determination results are plotted as a curve to produce continuous changes in energy from top to bottom. This method is used to calculate the energy of wells GC4, GC6, GC7, and GC8. The results of energy determination in some depths of well GC7 can be seen. However, this method cannot accurately and reasonably determine the energy of dolomite. To distinguish the energy of dolomites from that of other lithology associations, the energy of dolomites is assigned the lowest value (Fig. 3(a)). The energy change curve reveals that the Upper Ordovician has massive energy (Yijianfang Formation and first member of Yingshan Formation). In contrast, low energy dominates the upper part of the second member of the Yingshan Formation. Instead, the lower part of the second member of the Yingshan Formation and the upper part of the third member of the Yingshan Formation is characterized by an interaction of high, medium, and low energy, with the high-energy dominating. The lower part of the third member of the Yingshan Formation is made up of high and low energy. In the fourth member of the Yingshan Formation, the upper part is dominated by low energy, while the lower part is dominated by high energy. Unlike the energy changes in the Yingshan and Yijianfang formations, the energy in the Penglaiba Formation is primarily composed of low energy, with a small portion

Table 2 The results of parameters from gamma ray spectrometry by integrated superimposition method in different depths of Well GC7 (1 dolomite; 2 limestone; 3 low energy; 4 medium energy; 5 high energy; 0 Null; P1 = Parameter 1; P2 = Parameter 2)

Depth/m	Parameter				Calculation result					Final result
	U-K/ppm	Th/U(FRAC)	P1/ppm	P2/ppm	PE	U-K/ppm	P1/ppm	P2/ppm	Th/U(FRAC)	
5599.375	0.22	5.28	0.03	0.25	2	3	3	3	3	3
5599.5	0.25	5.06	0.03	0.28	2	3	3	3	3	3
5599.625	0.28	4.73	0.05	0.33	2	3	3	3	3	3
5599.75	0.23	5.05	0.04	0.27	2	3	3	3	3	3
5600.125	0.32	4.6	0.05	0.37	2	3	3	3	3	3
5600.25	0.36	4.18	0.08	0.43	2	3	3	3	3	3
5630.125	0.57	0.71	1.09	1.65	2	4	4	4	4	4
5631.125	0.69	0.47	1.57	2.26	2	4	4	4	4	4
5631.25	0.7	0.54	1.4	2.1	2	4	4	4	4	4
5631.375	0.69	0.6	1.28	1.97	2	4	4	4	4	4
5631.5	0.66	0.6	1.28	1.94	2	4	4	4	4	4
5635.125	0.45	0.78	0.97	1.42	2	4	3	4	4	4
5635.25	0.51	0.79	0.98	1.49	2	4	3	4	4	4
5635.375	0.56	0.78	1	1.56	2	4	4	4	4	4
5635.5	0.58	0.75	1.05	1.62	2	4	4	4	4	4
5635.625	0.57	0.7	1.12	1.69	2	4	4	4	4	4
5636.5	0.8	0.32	2.6	3.41	2	4	5	5	4	5
5636.625	0.87	0.3	2.83	3.7	2	4	5	5	5	5
5636.75	0.9	0.29	2.88	3.78	2	4	5	5	5	5

(*continued*)

Depth/m	Parameter				Calculation result					Final result
	U-K/ppm	Th/U(FRAC)	P1/ppm	P2/ppm	PE	U-K/ppm	P1/ppm	P2/ppm	Th/U(FRAC)	
5636.875	0.9	0.29	2.88	3.78	2	4	5	5	5	5
5637	0.87	0.29	2.9	3.77	2	4	5	5	5	5
6143.375	1.93	0.28	2.78	4.71	1	0	0	0	0	1
6143.5	1.68	0.3	2.71	4.39	1	0	0	0	0	1
6143.625	1.63	0.26	3.01	4.64	1	0	0	0	0	1
6143.75	1.67	0.23	3.36	5.03	1	0	0	0	0	1
6143.875	1.67	0.24	3.31	4.98	1	0	0	0	0	1
6144	1.75	0.21	3.81	5.56	1	0	0	0	0	1
6144.125	1.71	0.23	3.56	5.27	1	0	0	0	0	1
6144.25	1.74	0.25	3.26	4.99	1	0	0	0	0	1
6144.375	1.85	0.24	3.4	5.25	1	0	0	0	0	1
6144.5	1.98	0.22	3.83	5.8	1	0	0	0	0	1
6144.625	2.04	0.22	3.81	5.85	1	0	0	0	0	1
6144.75	1.85	0.22	3.74	5.59	1	0	0	0	0	1

Notes: U/(Th+K)-Th/KTh (referred to as Parameter 1/P1); U/(Th+K)-Th/KTh+ U-K (referred to as Parameter 2/P2); PE indicates electron density index. U, Th, K indicates corresponding content of radioactive elements.

of high energy in the middle and lower parts (Fig. 3(a)). The energy changes are well correlated with lithology associations, which adds to the validity of the determination results.

The statistics and analysis of thin sections in the Ordovician of the eastern Tarim Basin show that the dolomites are primarily composed of medium-crystalline and fine-crystalline dolomite. Therefore, the conclusions are that the energy of the sedimentary environment where the dolomites are deposited is medium-low energy.

Groundwater activity is closely related to increased U content in the permeable stratum. Because of its active chemical properties and solubility in water, U is easily migrated to the deep by groundwater along faults or fracture zones formed in the karst or tectonically active zone. Then, it is reduced to tetravalent U and precipitated under reducing conditions. As a result, the U content has a strong relationship with hydrodynamics. Furthermore, the high Th and K contents indicate a stable and low-energy humid sedimentary environment. Furthermore, the high U and K contents indicate a turbulent and high-energy sedimentary environment with a dry climate (Ruffell and Worden, 2000). As a result, in natural GRS, the U, Th, and K contents can reflect energy changes in the sedimentary environment. The analysis reveals that determining dolomite energy is challenging. Therefore, the dolomite is first determined. Following that, the energy of limestone is determined. U, Th/U, parameter1, and parameter2 are the most commonly used parameters for determining energy. Both parameters have already been mentioned. Based on the values from the determination parameters and parameters calibrated by cores or thin sections, the energy in the sedimentary environment where carbonates are deposited is divided into three categories: high, medium, and low energy. The precise parameter ranges are then displayed (Table 3). Through energy changes, the final transition of parameters can reflect the sedimentary environment.

The identification of lithology associations and determination of energy in the Ordovician of well GC4 depicts energy changes resulting from wireline logs in general, which not only reflects overall energy changes but also shows energy changes in detail (Figs. 3(b), 4(a), 4(b), 4(c), 4(d), 4(e), 5(b), 5(d), and 5(g)).

The dolomite content is highest in well GC8. As a result, identifying dolomites takes precedence. The determination of energy in limestone and the identification of lithology associations reveal alternate transitions of high and low energy (Figs. 3(c), 4(f), 4(g), 5(h), and 5(i)). The energy determination in well GC4 reveals that high energy dominates the upper part. In contrast, the middle section generally denotes low energy, followed by a small portion of an alternation transition between high and medium energy. The characteristics from middle part to upper part reveal increasing energy from upper Yingshan Formation to the Yijianfang Formation. The lower part is dominated by a series of thick dolomites, the energy of which is difficult to determine. As a result, energy determination focuses on limestones (Figs. 3(b), 4(a), 4(b), 4(c), 4(d), 4(e), 5(d), and 5(j)).

4.2 The determination of ancient sedimentary environment

The distribution of radioactive elements derived from

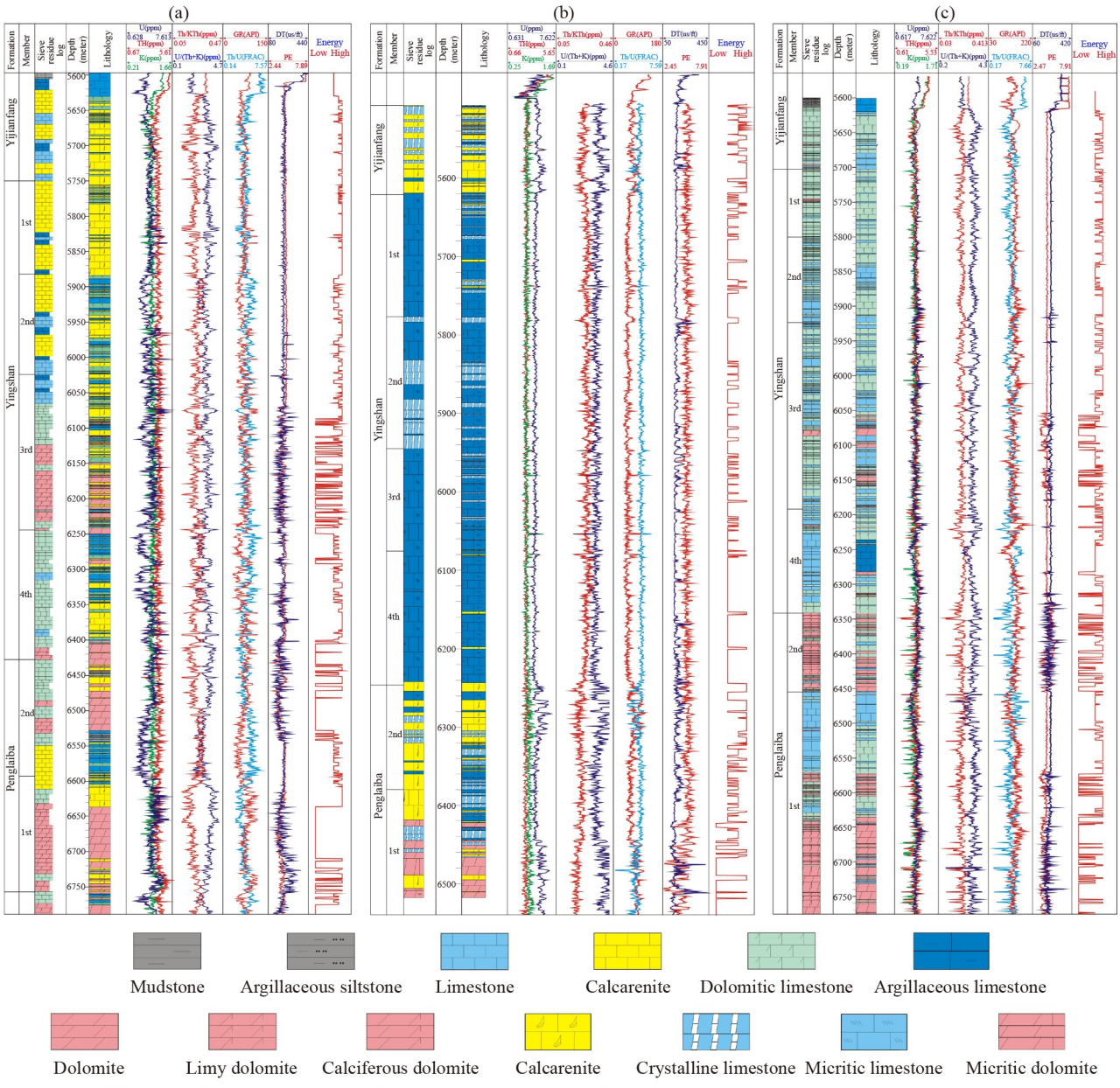

Notes: PE indicates electron density index. U, Th, K and associated assemblages indicates corresponding content of radioactive elements. U/(Th+K)-Th/KTh is referred to as Parameter 1 or P1 while U(Th+K)-Th/KTh+U-K is referred to as Parameter 2 or P2.

Fig. 3 The identification of lithology associations and determination of energy in the Ordovician based on wireline logs; (a) the interpretation of well GC7; (b) the interpretation of well GC 4; (c) the interpretation f well GC 8; Notes: PE indicates electron density index. U, Th, K and associated assemblages indicates corresponding content of radioactive elements. Among them, U/(Th + K)-Th/KTh is referred to as Parameter 1 or P1 while U/(Th + K)-Th/KTh + U-K is referred to as Parameter 2 or P2.

Table 3 The standard for determination of energy resulted from parameters of carbonate reservoirs in eastern Tarim Basin

Energy	Th/U(FRAC)	U/ppm	U-K/ppm	P1/ppm	P2/ppm
Low energy	0.2−0.8	<1.2	<0.85	<0.5	<1.5
Medium energy	0.8−1.2	1.2 −1.5	0.85−1.2	0.5−0.8	1.5−1.9
High energy	<1.2	>1.5	>1.2	>0.8	>1.9

Notes: U/(Th+K)-Th/KTh (referred to as Parameter 1/P1); U/(Th+K)-Th/KTh+ U-K (referred to as Parameter 2/P2); PE indicates electron density index. U, Th, K indicates corresponding content of radioactive elements.

natural GRS, such as U, Th, and K, not only aids in energy determination but also in revealing ancient sedimentary environments using thin sections, cores, and seismic data sets. In general, the Th and K content in sedimentary rocks decrease with grain size. Th and mudstone content are linearly related. The high Th and K content indicates a stable and humid sedimentary environment with low energy. In contrast, the high U content indicates a dry sedimentary environment. Furthermore, U content and hydrodynamics are linearly

related. The carbonates were deposited in the eastern Tarim Basin during the Middle-Lower Ordovician. It is dominated by limestone (primarily calcarenite) in the upper Yingshan Formation and the Yijianfang Formation (Figs. 2, 5(a), 5(d), 5(e), 5(k), and 5(l)). However, dolomite (primarily granular and limy dolomite) predominates in the lower Yingshan Formation and Penglaiba Formation (Figs. 2, 5(c), 5(f), 5(i), and 5(j)). The interpretation of seismic sections aid in determining that it is a typical carbonate platform (Figs. 6, 4(h), 4(i), 5(i), and 5(l)).

The study area's facies are mostly made up of platform facies and platform margin facies. The energy curve from well GC7 shows that it has high energy from the upper part of the third member of the Yingshan Formation to the Yijianfang Formation. The concentration of the single radioactive element Th is exceptionally high. The values of the single radioactive elements U and K vary considerably. The composite parameter values (parameters 1 and 2) are relatively high, while the composite parameter values Th/U are relatively low. These characteristics reveal a dry sedimentary environment with turbulent shallow water. Calcarenite dominates the lithology, deposited in a psammitic shoal in the platform margin facies. It is distinguished by the interaction of high, medium, and low energy from the lower part of the third member of the Yingshan Formation to the Penglaiba Formation. U values vary significantly, followed by the composite parameter (Th/U). It generally denotes a dry, active sedimentary environment with various lithology associations. Dolomitic limestone, micrite, granular dolomite, and limy dolomite are typical lithologies in platform margin facies, reflecting psammitic shoal and interbank sea (Fig. 3(a)). The wireline properties of well GC8 are similar to those of well GC7 (Fig. 3(c)). The energy curve from well GC6 demonstrates the interaction of high and low energy from the upper part of the second member of the Yingshan Formation to the Yijianfang Formation. In contrast, it is distinguished by low energy from the second to third members of the Yingshan Formation. The values of Th, U, and K vary significantly, indicating an unstable sedimentary environment with transition characteristics from high to low energy. The lithology comprises micrite and fine-crystalline limestone deposited between the platform margin facies and the platform facies (Fig. 7).

The Ordovician well correlation shows that the gentle carbonate slope gradually incorporates into the carbonate platform margin with obvious slope during the Early Ordovician in the study area (Fig. 8). On the platform margin's high-energy belts, the platform marginal reef-shoal is well-developed. The platform margin's outer side

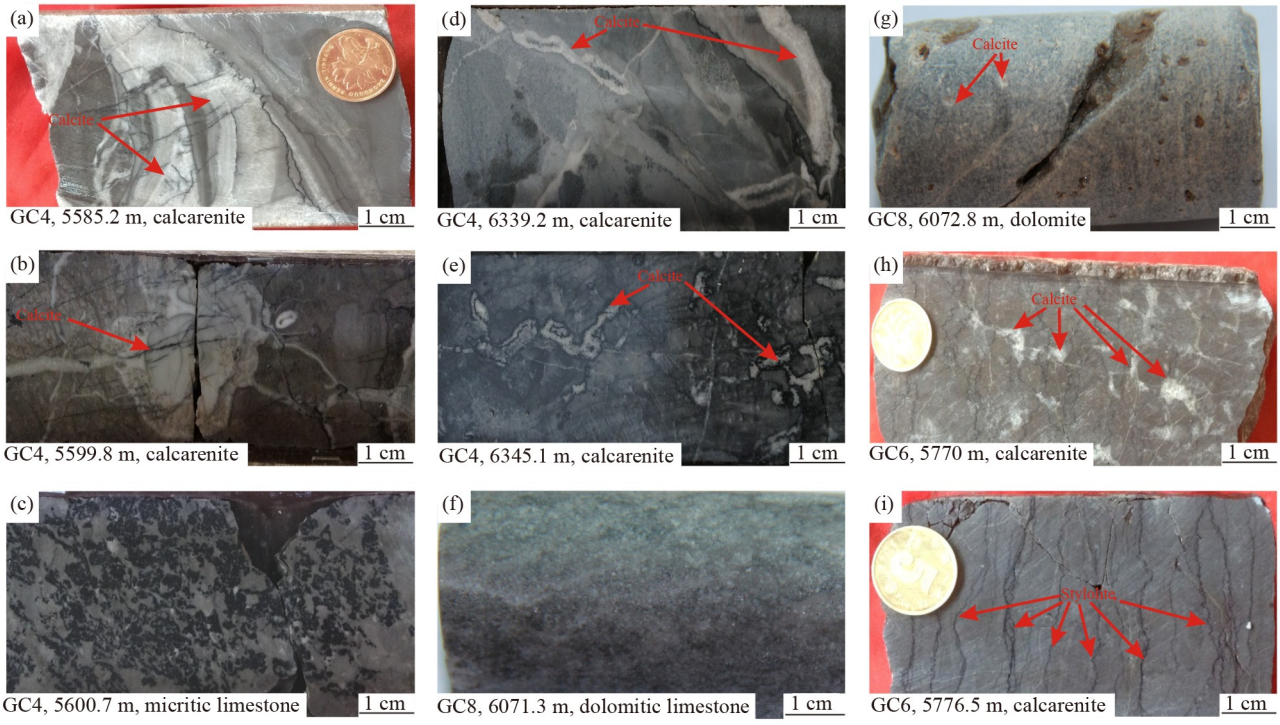

Fig. 4 The cores showing the characteristics of lithology in the Ordovician (including Penglaiba Formation, Yingshan Formation, and Yijianfang Formation): (a) calcarenite filled with calcite from well GC4 in depth of 5585.2 m; (b) calcarenite filled with calcite from well GC4 in depth of 5599.8 m; (c) micritic limestone from well GC4 in depth of 5600.7 m; (d) calcarenite filled with calcite from well GC4 in depth of 6339.2 m; (e) calcarenite filled with calcite from well GC4 in depth of 6345.1 m; (f) dolomitic limestone from well GC8 in depth of 6071.3 m; (g) dolomite from well GC8 in depth of 6072.8 m; (h) calcarenite filled with calcite and stylolite from well GC6 in depth of 5770 m; (i) calcarenite filled with stylolite from well GC6 in depth of 5776.5 m.

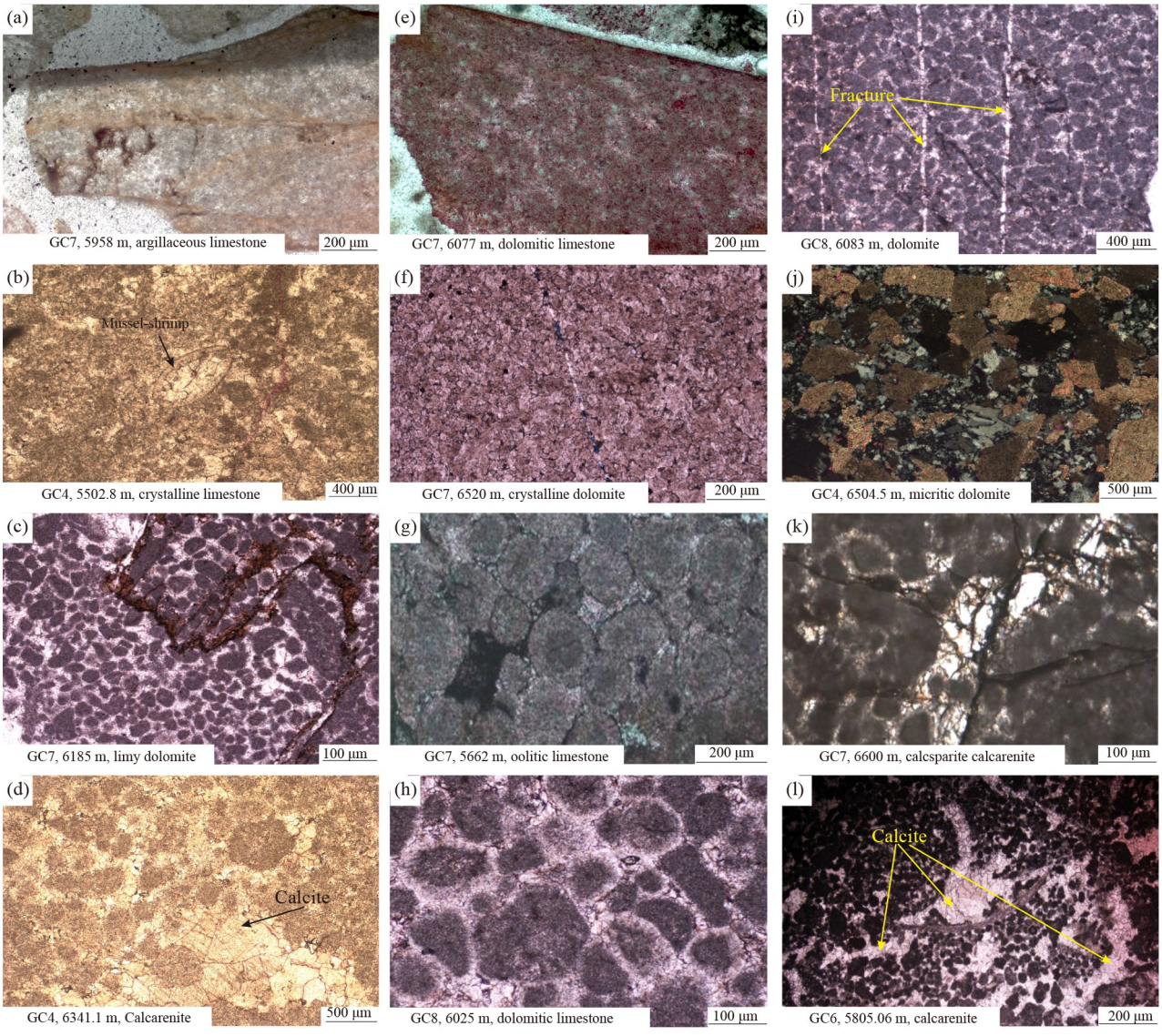

Fig. 5 The thin sections showing the characteristics of lithology in the Ordovician (including Penglaiba Formation, Yingshan Formation, and Yijianfang Formation): (a) argillaceous limestone from well GC7 in depth of 5958 m; (b) crystalline limestone from well GC4 in depth of 5502.8 m; (c) limy dolomite from well GC7 in depth of 6185; (d) calcarenite from well GC4 in depth of 6341.1 m; (e) dolomitic limestone from well GC7 in depth of 6077 m; (f) crystalline dolomite from well GC7 in depth of 6520 m; (g) oolitic limestone from well GC7 in depth of 5662 m; (h) dolomitic limestone from well GC8 in depth of 6025 m; (i) dolomite from well GC8 in depth of 6083 m; (j) micritic dolomite from well GC4 in depth of 6504.5 m; (k) calcsparite calcarenite from well GC7 in depth of 6600 m; (l) calcarenite from well GC6 in depth of 5805.06 m.

develops a neritic a shelf and shelf slope. However, the platform margin is usually quite visible, evolving into a steep platform margin during the middle-late Ordovician (Fig. 8). The energy of the sedimentary environment in the first member of the Penglaiba Formation is low, with low Th and K values. Instead, it is distinguished only by high energy in well GC8 and high parameters 1 and 2 values, indicating a relatively deep-water depth. The energy of the sedimentary environment decreases toward the platform in the second member of the Penglaiba Formation. In comparison to the first member of the Penglaiba Formation, the study area evolves into a locally drowned platform in the second member. It demonstrates low energy in the fourth member of the Yingshan Formation with low values of Th/U and Th, implying that it was a platform facies during transgression. The energy in the third, second, and first members of the Yingshan Formation is generally high, with low Th and K values and high values of parameters 1 and 2, indicating an open platform (platform facies)-foreslope (platform margin facies). The Yijianfang Formation's energy is a mix of high and low energy, indicating an evolutionary transition from a foreslope in platform margin facies to a locally drowned platform in platform facies. The integrated analysis of energy and sedimentary environment produced by natural GRS shows that sea level rises in

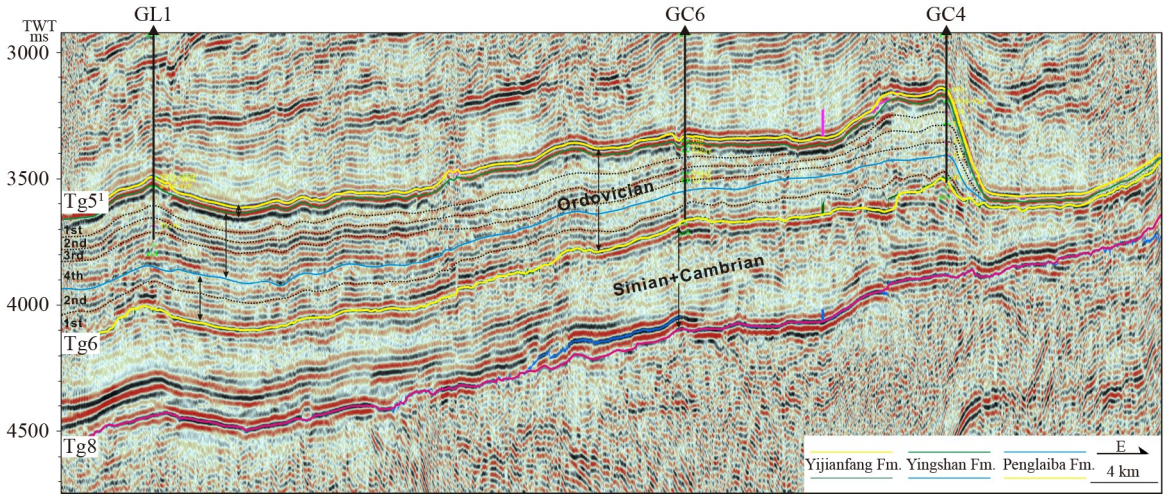

Fig. 6 The interpretation of seismic section showing the characteristics of strata distributions and seismic reflections of different formations (including Penglaiba Formation, Yingshan Formation and Yijianfang Formation) in the Ordovician.

general during the Early Ordovician (Penglaiba Formation-fourth member of the Yingshan Formation) and falls during the middle-late Ordovician (third member of Yingshan Formation-Yijianfang Formation).

5 Discussion

The novel approach of natural GRS log is employed to investigate the Ordovician deep-buried carbonates of the eastern Tarim Basin to reveal genetic relationships between radioactive elements such as Th, U, K, and sedimentary environment and associated energy. The natural GRS log is produced by artificially measuring changes in radioactive element concentration and gamma-ray intensity in rock records during nuclear decay. The GRS log has become widely available and used in the energy industry (Davies and Elliott, 1996; Ruffell and Worden, 2000; Lima et al., 2005; Ghosal et al., 2020). This is because it is capable of reconstructing sedimentary environments and paleoclimates in sedimentary basins. Furthermore, it can reveal the hydrodynamics, water depth, and energy of sedimentary environments (Chen and Zha, 2004; Lima et al., 2005; Ghosal et al., 2020).

Because argillaceous content and radioactive element concentration are linearly related, the natural GRS log is used to effectively determine argillaceous content in rock records based on changes in the radioactive element concentration (Th, U, and K). Furthermore, the ratio of thorium/uranium content (Th/U) and thorium/potassium content (Th/K) can be used to calculate changes in the sedimentary environment and relative ancient water depth (Davies and Elliott, 1996; Yang et al., 2003; Zhang et al., 2006).

Modern statistical studies on the interpretation of natural GRS logs show that U chemical properties are relatively active (Davies and Elliott, 1996; Chen and Zha, 2004). The reduction and adsorption of U by organic matter during the diagenetic process is the primary mechanism of U enrichment in sedimentary rocks. As a result, U enrichment in sedimentary rocks reflects a deteriorating environment. Th has a more stable chemical property than U (Liu et al., 2000; Lima et al., 2005; Zhang et al., 2006). As a result, three sedimentary environments can be distinguished based on the change in Th/U value: when Th/U > 7, it generally indicates shallow water under oxidation conditions or in an exposed environment. When 2 < Th/U < 7 is present, it indicates an interactive neritic shelf sedimentary environment with transitional reduction-oxidation conditions. Th/U < 2 generally indicates deep-water under strong reduction conditions, with sediments characterized by gray or green shale (Wang and Zhu, 2002; Wang, 2004; Lima et al., 2005; Ghosal et al., 2020). Changes in the Th/K value of sedimentary rocks can also indicate changes in the sedimentary environment and water depth. The high Th/K value indicates that the stratum has been exposed to weathering. The Th/K value of long-exposed large-scale weathering crust is frequently greater than 7; low Th/K values indicate deep-water environments with low-energy reduction conditions (Ruffell and Worden, 2000; Zhang et al., 2006; Ghosal et al., 2020).

6 Conclusions

The integrated superposition method produced effective and fruitful results in determining the ancient sedimentary environment and associated energy in deep-buried marine carbonates based on natural GRS logs from the Ordovician in the eastern Tarim Basin.

1) Analyzing the energy and radioactive element distribution can objectively reflect the sedimentary

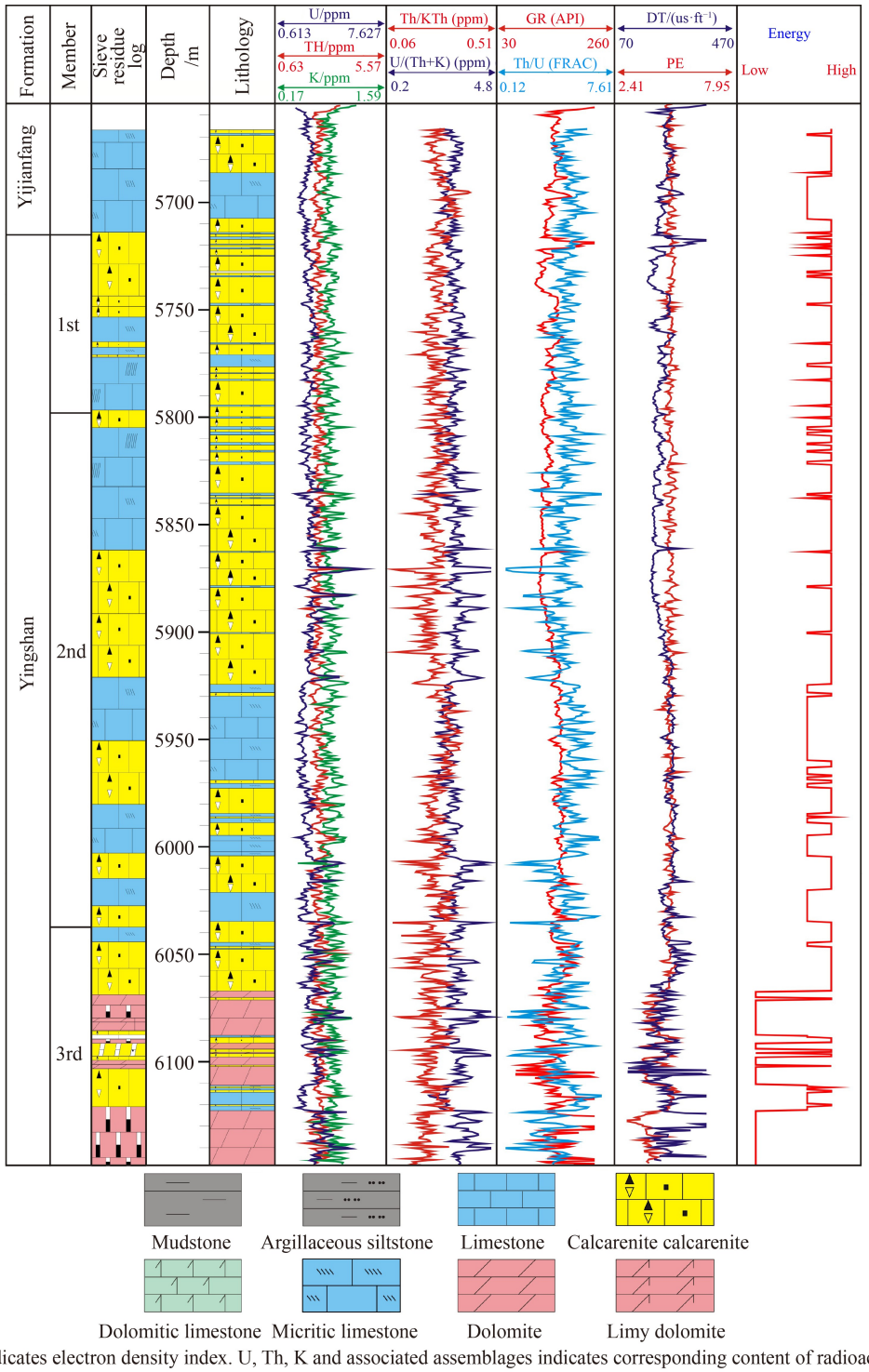

Notes: PE indicates electron density index. U, Th, K and associated assemblages indicates corresponding content of radioactive elements. Among them, U/(Th+K)-Th/KTh is referred to as Parameter 1 or P1 while U/(Th+K)-Th/KTh+U-K is referred to as Parameter 2 or P2.

Fig. 7 The identification of lithology associations and determination of energy in the Ordovician based on wireline logs in well GC6; Notes: PE indicates electron density index. U, Th, K and associated assemblages indicates corresponding content of radioactive elements. Among them, U/(Th + K)-Th/KTh is referred to as Parameter 1 or P1 while U/(Th + K)-Th/KTh + U-K is referred to as Parameter 2 or P2.

environment. Furthermore, lithology associations and seismic reflections can be used to determine the Ordovician sedimentary environment in the eastern Tarim Basin.

2) During the Ordovician, the carbonate platform dominated the sedimentary facies in the eastern Tarim Basin. From the Penglaiba Formation to the Yijianfang Formation, the sedimentary cycle transitions from

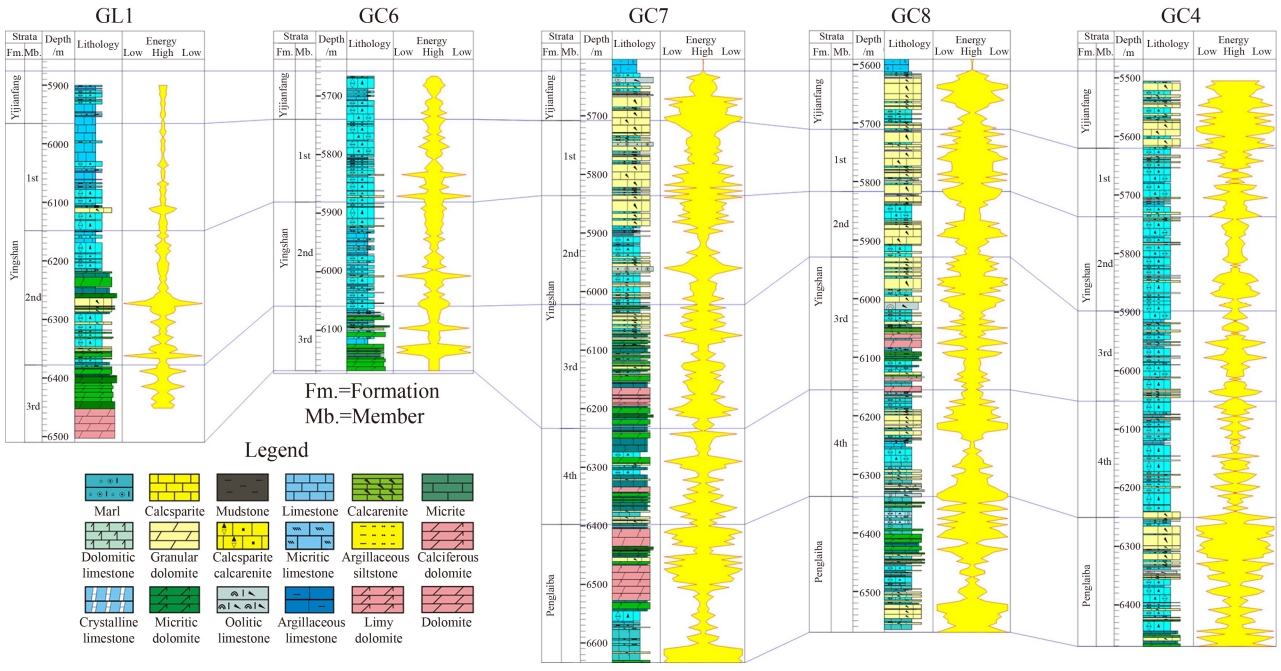

Fig. 8 The well correlation (well GL1-well GC6-well GC7-well GC8-well GC4) showing the distribution of strata, lithology association and sedimentary energy in the Ordovician in eastern Tarim Basin (please see Fig. 1 for well location).

transgression to regression. The platform margin facies are deposited in wells GC4, GC7, and GC8. Instead, the well GC6 is in the transition zone between the foreslope in the platform margin facies and the open platform in the platform facies.

3) Based on well correlation from wells GC4, GC8, GC7, GC6, and GL1, the facies generally change from foreslope in platform margin facies to open platform and restricted platform in platform facies.

4) In summary, using lithology associations and seismic reflections, the natural GRS log can be used to determine ancient sedimentary environments and associated energy. The workflows described in the manuscript can provide solid insights and useful guidance for determining the sedimentary environment and associated energy in deep-buried carbonate reservoirs. Because the petroleum exploration in deep-buried carbonate reservoirs has important scientific implications in today's oil industry.

Acknowledgments The Exploration and Development Research Institute, Daqing Oilfield Company, PetroChina is thanked for providing the data sets; then the authors gratefully acknowledge financial support from the Key Droject the National Natural Foundation of China (No. 42330810), the National Natural Science Foundation of China (Grant No. U19B6003-01-01) and the State Key Program of the National Natural Science Foundation of China (No. 41130422). Furthermore, anonymous reviewers and executive editor are thanked for constructive comments and helpful inputs which helped significantly improve the manuscript.

Data availability statement The data that support the findings of this study are available on request from the corresponding author. The data are not publicly available due to privacy or ethical restrictions.

Competing interests The authors declare that they have no competing interests.

References

Adamu A, Ologe O, Ahmed A L, Sunusi A Y (2020). Characterisation for radioelements over an escarpment feature(S): a case study of the Duku-Tarasa Gwandu ridge area of Birnin Kebbi NW Nigeria. Int J Geosci, 11(8): 529–543

Chen Y, Yuan L W, Zhou C L, Liu Z C (2001). Quaternary Palaeoclimatic changes recorded by natural gamma logging curve in Qaidam Basin. J Palaeogeogr, 5: 29–37 (in Chinese)

Chen Z H, Zha M (2004). Application of uranium curve to paleoenvironment inversion in sedimentary basin. J China U Petrol (Nat Sci), 28: 11–15 (in Chinese)

Chi S L (2003). On discussion of concentration of radioelements in the earth's crust. Earth Sci J China U Geosci, 28: 17–20 (in Chinese)

Davies S J, Elliott T (1996). Spectral gamma ray characterization of high resolution sequence stratigraphy: examples from Upper Carboniferous fluvio-deltaic systems, County Clare, Ireland. Spec Publ Geol Soc Lond, 104(1): 25–35

Dong S L, Li Z, Xu J Q, Gao J, Guo C T (2014). Detrital zircon U-Pb geochronology and Hf isotopic compositions of Middle-Upper Ordovician sandstones from the Quruqtagh area, eastern Tarim Basin: implications for sedimentary provenance and tectonic evolution. Chin Sci Bull, 59(10): 1002–1012 (in Chinese)

Ehrenberg S N, Svana T A (2001). Use of gamma-ray signature to interpret stratigraphic surfaces in carbonate strata: an example from the Finnmark carbonate platform (Carboniferous-Permian), Barents Sea. AAPG Bull, 85: 295–308

Feng W M, Xie Y, Liu J Q, Lin J S, Chen G, Zhao Z (2016). Sedimentological significance of natural gamma ray logging data of

marine carbonate: a case of the well L1 of Qingxudong Formation, Lower Cambrian in southeast Sichuan Basin. Marine Geo Quatern Geo, 36: 165–172 (in Chinese)

Feng Z Z, Bao Z D, Wu M B, Jin Z K, Shi X Z, Luo A R (2007). Lithofacies palaeogeography of the Ordovician in Tarim area. J Palaeogeogr, 9: 447–460 (in Chinese)

Gao D, Lin C S, Hu M Y, Huang L L (2016). Using spectral gamma ray log to recognize high-frequency sequences in carbonate strata: a case study from the Lianglitage Formation from well T1 in Tazhong area, Tarim Basin. Acta Sediment Sin, 34: 707–715 (in Chinese)

Ghasemi-Nejad E, Ardakani E P, Ruffell A (2010). Palaeoclimate change recorded in Upper Cretaceous (Albian-Cenomanian) Kazhdumi Formation Borehole SPECTRAL Gamma-Ray Logs, South Pars Gas field, Persian Gulf. Palaeogeogr Palaeoclimatol Palaeoecol, 291(3–4): 338–347

Ghosal S, Agrahari S, Banerjee S, Chakrabarti R, Sengupta D (2020). Geochemistry of the heavy mineral sands from the Garampeta to the Markandi beach, southern coast of Odisha, India: implications of high contents of REE and radioelements attributed to Placer Monazite. J Earth Syst Sci, 129(1): 152

Guo Y F, Fu S Y, Du H L, Wang B C (1996). Relations between natural gamma ray spectrometry and lithologic parameters in Sanzhao region of Songliao Basin. Acta Petrol Sin, 4: 24–28 (in Chinese)

Han C W, Ma P L, Zhu D X, Du D W, Xiao J, Liu X M (2009). The tectonic characteristics and its evolution in the Eastern Tarim Basin, Xinjiang. Geotectonica et Metallogenia, 33: 131–135 (in Chinese)

He D F, Jia C Z, Li D S, Zhang C J, Meng Q R, Shi X (2005). Formation and evolution of polycyclic superimposed Tarim Basin. Oil Gas Geol, 26: 64–77 (in Chinese)

He F, Lin C S, Liu J Y, Zhang Z L (2016). Carbonate rock sedimentation and its main-controlling factors in Gucheng. Special Oil Gas Reservoirs, 23: 17–21 (in Chinese)

He F, Lin C S, Liu J Y, Zhang Z L, Zhang J L, Yan B, Qu T L (2017). Migration of the Cambrian and Middle-Lower Ordovician carbonate platform margin and its relation to relative sea level changes in southeastern Tarim Basin. Oil Gas Geol, 38: 711–721 (in Chinese)

Koptíková L, Bábek O, Hladil J, Kalvoda J, Slavik L (2010). Stratigraphic significance and resolution of spectral reflectance logs in Lower Devonian carbonates of the Barrandian area, Czech Republic; a correlation with magnetic susceptibility and gamma-ray logs. Sediment Geol, 225(3–4): 83–98

Laborde A, Barrier L, Simoes M, Li H, Coudroy T, Van der Woerd J, Tapponnier P (2019). Cenozoic deformation of the Tarim Basin and surrounding ranges (Xinjiang, China): a regional overview. Earth Sci Rev, 197: 102891

Lima A, Albanese S, Cicchella D (2005). Geochemical baselines for the radioelements K, U, and Th in the Campania region, Italy: a comparison of stream-sediment geochemistry and gamma-ray surveys. Appl Geochem, 20(3): 611–625

Lin C S, Yang H J, Cai Z Z, Yu B S, Chen J Q, Li H, Rui Z F (2013). Evolution of depositional architecture of the Ordovician carbonate platform in the Tarim Basin and its responses to basin processes. Acta Sedimentologica Sinica, 31: 907–919 (in Chinese)

Lin C S, Yang H J, Liu J Y, Rui Z F, Cai Z Z, Li S T, Yu B S (2012). Sequence architecture and depositional evolution of the Ordovician carbonate platform margins in the Tarim Basin and its responses to tectonism and sea-level change. Basin Res, 24(5): 559–582

Liu G, Zhou D S (2007). Application of microelements analysis in identifying sedimentary environment-Taking Qianjiang Formation in the Jianghan Basin as an example. Petroleum Geol Experiment, 29: 307–311 (in Chinese)

Liu W, Zhang X Y, Gu J Y (2009). Sedimentary environment of Lower-Middle Ordovician Yingshan Formation in Mid-Western Tarim Basin. Acta Sediment Sin, 27: 435–442 (in Chinese)

Liu Z C, Chen Y, Yuan L W, Zhou C L, Wang Y J, Li J Q, Yang P, Xi P (2000). Applications of natural gamma logging curve inversion 2.85Ma B. P. to the ancient climate change. Sci China Ser D Earth Sci, 30: 609–618 (in Chinese)

Ruffell A, Worden R H (2000). Paleoclimate analysis using spectral gamma-ray data from the Aptian (Cretaceous) of southern England and southern France. Palaeogeogr Palaeoclimatol Palaeoecol, 155(3–4): 265–283

Tang L J, Jia C Z, Jin Z J, Ma Z J (2003). The main tectonic characteristics of superimposed basins, northwest China. Earth Sci Front, 10: 118–124 (in Chinese)

Wang G, Fan T L, Liu H L (2014a). Characteristics and evolution of Ordovician carbonate platform marginal facies in Tazhong-Gucheng Area, Tarim Basin. Geoscience, 28: 995–1007 (in Chinese)

Wang J B, Zhu L P (2002). Grain-size characteristics and their paleo-environmental significance of Chen Co Lake sediments in southern Tibet. Prog Geogr, 21: 459–467 (in Chinese)

Wang Q (2004). Application of GR spectroscopy log in stratigraphic classification of the Ordovician formation in Tahe oil-field. Geophys Prospect Pro Petrol, 43: 504–507 (in Chinese)

Wang Z M, Yang H J, Qi Y M, Chen Y Q, Xu Y L (2014b). Ordovician gas exploration breakthrough in the Gucheng lower uplift of the Tarim Basin and its enlightenment. Nat Gas Ind, 34: 1–9 (in Chinese)

Wang Z Y, Han J, Xiong Y X, Sun C H, Yu H F (2011). Depositional framework of Early-Middle Ordovician in Tazhong-Gucheng Area in Tarim Plate. Xinjiang Petrol Geol, 32: 228–230 (in Chinese)

Wu B, He D F, He J Y, Liu L F (2018). Restoration of total thickness eroded by main unconformities in Tadong Area, Tarim Basin and genetic mechanism. Marine Geol Front, 34: 56–65 (in Chinese)

Wu B, He D F, Sun F Y (2015). Fault characteristics and genetic mechanism of the Lower Paleozoic in Gucheng Lower Uplift, Tarim Basin. Nat Gas Geosci, 26: 871–879 (in Chinese)

Wu G G, Li H Q, Chu B J, Xia B, Wang H, Pu G M (2002). Geotectonic evolution and petroleum accumulation in East Tarim. Geotectonica et Metallogenia, 26: 229–234 (in Chinese)

Wu X S, Guo J J, Huang Y J, Fu J W (2011). Well logging proxy of the Late Cretaceous palaeoclimate change in Songliao Basin. J Palaeogeogr, 2: 103–110 (in Chinese)

Yang P, Chen Y, Liu Z C (2003). Application of gamma ray log to study on palaeoclimate and sedimentary environments of the Jurassic in Qaidam Basin. J Palaeogeogr, 5: 94–101 (in Chinese)

Yang X F, Lin C S, Yang H J, Peng L, Liu J Y, Xiao T J, Tong J Y,

Wang H P, Li H P (2010). Application of natural gamma ray spectrometry in analysis of Late Ordovician carbonate sequence stratigraphic analysis in middle Tarim Basin. Oil Geophys Prospect, 45: 384–391 (in Chinese)

Zhang J L (2017). Carbonate sequence sedimentary evolution and control of sea level: a case study of Ordovician in the Gucheng area, Tarim Basin. Nat Gas Ind, 37: 46–53 (in Chinese)

Zhang S Y, Fan Y R, Li H Y (2006). Karst carbonate reservoir division and contrast based on natural gamma ray spectrometry logging in Tahe Oilfield. J China U Petrol, 30: 35–41 (in Chinese)

Zhang Y J, Zhang X J, Zhang Z W, Cao Y Q (2020). Characteristics and their controlling factors of Ordovician dolomite reservoir in Yingshan Formation in Gucheng Area. Petrol Geol Oilfield Develop Daqing, 39: 1–8 (in Chinese)

Zhang Y, Li Q, Zheng X P, Li Y L, Shen A J, Zhu M, Xiong R, Zhu K D, Wang X D, Qi J S, Zhang J L, Shao G M, She M, Song X, Sun H H (2021). Types, evolution and favorable reservoir facies belts in the Cambrian-Ordovician platform in Gucheng-Xiaotang area, eastern Tarim Basin. Acta Petrol Sin, 42: 447–465 (in Chinese)

Zhao Z J, Chen X, Pan M, Wu X N, Zheng X P, Pan W Q (2010). Milankovitch cycles in the Upper Ordovician Lianglitage Formation in the Tazhong-Bachu Area, Tarim Basin. Acta Geol Sin, 84: 518–536 (in Chinese)